Low-Cost Solar
Array Project
5101-106

DOE/JPL-1012-21
Distribution Category UC-63b

On the Modeling of Silane Pyrolysis in a Continuous Flow Reactor

Ananda K. Praturi
Ravi Jain
George C. Hsu

Jet Propulsion Laboratory
California Institute of Technology
Pasadena, California

DISCLAIMER

ABSTRACT

Silane pyrolysis in a continuous flow pyrolyzer is a simple process that is currently being developed for producing solar cell grade silicon. The process involves complex phenomena, however, including thermal decomposition of silane, nucleation and growth of silicon particles, and mass and heat transfer. Modeling the effects of transport phenomena on silane pyrolysis in a continuous flow pyrolyzer is discussed in this report. One- and two-dimensional models are developed to predict velocity, temperature, and concentration profiles in the reactor. The one-dimensional model has been implemented as a computer code.

NOMENCLATURE

A_1	frequency factor for homogeneous pyrolysis of silane, sec^{-1}
A_2	frequency factor for heterogeneous pyrolysis of silane, sec^{-1}
C	concentration of total gas phase, g-mole/cm^3
C_h	concentration of molecular hydrogen, g-mole/cm^3
C_s	concentration of silicon vapor, g-mole/cm^3
C_{si}	concentration of silane gas, g-mole/cm^3
$C_{si,s}$	concentration of silane on surface, g-mole/cm^3
C_p	specific heat of gas mixture at constant pressure, cal/g-mole^oK
C_v	specific heat of gas mixture at constant volume, cal/g-mole^oK
$C_{si,m}$	cross-sectional mean of silane concentration, g-mole/cm^3
$C_{h,m}$	cross-sectional mean of hydrogen concentration, g-mole/cm^3
$C_{si,i}$	initial value of silane concentration, g-mole/cm^3
$C_{h,i}$	initial value of hydrogen concentration, g-mole/cm^3
d_p	particle diameter, cm
D_{AB}	binary diffusivity for silane hydrogen mixture, cm^2/sec
g	gravitational acceleration, 981 cm/sec^2
h	heat transfer coefficient, cal/cm^2 sec ^oK
k	thermal conductivity of gas mixture, gm-cm/sec^3 ^oK
k_1	specific reaction rate constant for homogeneous pyrolysis of silane, sec^{-1}
k_2	specific reaction rate constant for heterogeneous pyrolysis of silane, sec^{-1}
k_m	mass transfer coefficient, cm/sec
M_{si}	molecular weight of silane, gm/g-mole
M_h	molecular weight of hydrogen, gm/g-mole
M_s	atomic weight of silicon, gm/g-atom
m	mass per seed particle, gm
n	number concentration of seed particles, cm^{-3}

n_i initial number concentration of seed particles, cm^{-3}

N_{si} flux of silane, g-mole/cm^2sec

N_h flux of hydrogen, g-mole/cm^2sec

$N_{si,H}$ rate of silane pyrolysis by homogeneous mechanism, g-mole/cm^3sec

P pressure, dynes/cm^2

R_r reactor radius, cm

r radial coordinate, cm

R gas constant, 8.314×10^7 gm cm^2/sec^2 g-mole ^oK

s surface area per seed particle, cm^2

t time, sec

T temperature of the gas stream, ^oK

T_m axial mean temperature of the gas stream, ^oK

T_i initial temperature of the gas stream, ^oK

T_w wall temperature, ^oK

V_r radial velocity of gas stream, cm/sec

V_z axial velocity of gas stream, cm/sec

$V_{z,m}$ axial mean velocity of gas stream, cm/sec

$V_{z,i}$ initial axial mean velocity of gas stream, cm/sec

x_A mole fraction of silane

x_B mole fraction of hydrogen

z axial coordinate, cm

Greek Symbols

ρ density of gas mixture, gm/cm^3

ϵ void fraction in the reactor

λ heat of reaction (includes heat of condensation), cal/g-mole

ΔE_1 activation energy for homogeneous silane pyrolysis, cal/g-mole

ΔE_2 activation energy for heterogeneous silane pyrolysis, cal/g-mole

μ viscosity of gas mixture, poise

CONTENTS

SECTION I

INTRODUCTION AND THEORY

Silane pyrolysis is one of a number of approaches to the production of polycrystalline silicon for use in the fabrication of solar cells. A continuous flow pyrolyzer (CFP) is one of the reactors that is being studied for use in the formation and growth of silicon particles by this method. The mechanisms of silicon particle formation and growth involve silane pyrolysis and silicon nucleation. The kinetic mechanisms are independent of reactor configurations; the steps involved have been modeled by Praturi (Reference 1) and by Praturi et al (Reference 2). The effect of transport processes (momentum, heat and mass transfer) on the rate of silicon particle formation and growth, however, is very much dependent on the reactor design and reactor operating conditions. It is the purpose of the present study to model the effects of transport processes on the overall rate of silicon production in the continuous flow pyrolyzer.

A. MECHANISMS OF SILICON PRODUCTION

Basically, there are two mechanisms by which silicon particles are produced from silane pyrolysis. These are referred to as the homogeneous and the hetergeneous mechanisms.

1. The Homogeneous Mechanism

The homogeneous mechanism consists of homogeneous pyrolysis of silane and homogeneous nucleation of silicon vapor to form silicon nuclei. The rate of these two steps depends on the temperature of the gas stream, concentration of silane, and the supersaturation of silicon vapor. The effects of transport processes on the homogeneous mechanism are limited to determining the velocity, temperature, and concentration profiles in the CFP. The rate of silicon production by the homogeneous mechanism can be estimated quantitatively by a first-order Arrhenius type equation* (Reference 3):

$$\frac{-dC_{si}}{dt} = k_1 C_{si}$$

$$= A_1 e^{-\Delta E_1/RT} C_{si} \qquad (1)$$

*Symbols and units for all equations are defined in NOMENCLATURE (in front of report).

The depletion of silane by the homogeneous mechanism can therefore be accounted for simply in the mass balances. The homogeneous mechanism yields solid silicon nuclei. The size and distribution of these nuclei can be estimated from the homogeneous nucleation theory (Reference 4).

2. The Heterogeneous Mechanism

The heterogeneous mechanism provides the means for silicon particle growth. This mechanism consists of mass transport of silane to the particle surface, heterogeneous pyrolysis of silane on particles, and heterogeneous nucleation of silicon on the particles. When the heterogeneous pyrolysis and nucleation steps occur at much higher rates than the mass transport of silane, the overall rate of silicon particle growth can be given by the rate of mass transport. It is this case of mass-transfer-limited particle growth, in which the pryolysis and nucleation steps occur at equilibrium or estremely high rates, that is modeled in this study. Modeling of particle growth when either the pyrolysis step or the nucleation step is controlling is described in References 1 and 2. Therefore, only the effects of transport processes on the mass transfer of silane to particle surface need to be considered in order to predict the overall particle growth rate. The rate of combined pyrolysis and nucleation steps in the heterogeneous mechanism can be assumed to be given by the first-order Arrhenius type equation (Reference 5):

$$\frac{-dC_{si}}{dt} = k_2 C_{si}$$

$$= A_2 e^{-\Delta E_2/RT} C_{si} \qquad (2)$$

Since this rate is at least an order of magnitude higher (implicit assumption) than the rate of mass transport, it can safely be assumed that the concentration of silane on the particle surface vanishes to zero.

Clearly, therefore, it is the transport processes in the CFP that need to be modeled in order to predict the rate of new silicon nuclei formation and the particle growth rate. The processes of momentum, mass, and heat transfer in the CFP occur simultaneously and are best described by their respective conservation equations. In the general case, these conservation equations are non-linear partial differential equations, and the general simultaneous solution would be extremely difficult, if not impossible, to obtain. Simplifications have to be made to obtain solutions to the simultaneous non-linear, partial differential equations.

B. PROCESS DESCRIPTION

The process of silicon production in a CFP is shown schematically in Figure 1-1. In this process, a gas mixture containing silane and hydrogen and fine silicon particles (0.1-50μ) are fed to the tubular reactor. The reactor is heated through the walls to give a gas temperature of 400°-1000°C. At these temperatures silane is thermally decomposed to produce silicon by the homogeneous and heterogeneous mechanisms.

C. MODEL ASSUMPTIONS AND OBJECTIVE

Modeling of the process of silane pyrolysis in the CFP is based on the following set of assumptions:

(1) The steady state prevails in the entire length of the CFP with respect to momentum, heat, and mass transfer processes.

(2) The overall rate of silane pyrolysis and silicon nucleation steps (in both the homogeneous and heterogeneous mechanisms) can be given by a first-order Arrhenius type equation. This implies that the nucleation step is faster than the pyrolysis step.

(3) Heat is transferred through the reactor walls to the gas stream at a constant wall temperature T_w. The gas stream enters the reactor at a constant inlet temperature T_i.

(4) In the reactor the gases and the silicon particles are in thermal equilibrium and hence both are the same temperature T.

(5) The silicon particles are small enough in size and have a low enough number density so that they follow fluid motions and do not affect flow patterns or heat and mass transfer rates.

(6) Diffusional transfer in the reactor can be described as binary (silane, hydrogen) counter diffusion.

The objective of this modeling effort is to predict 1) the rate of silicon production, 2) the rate of silicon particle growth, and 3) the rate of silicon deposition on the reactor walls for given operating conditions of the CFP in the case of transport limited silane pyrolysis.

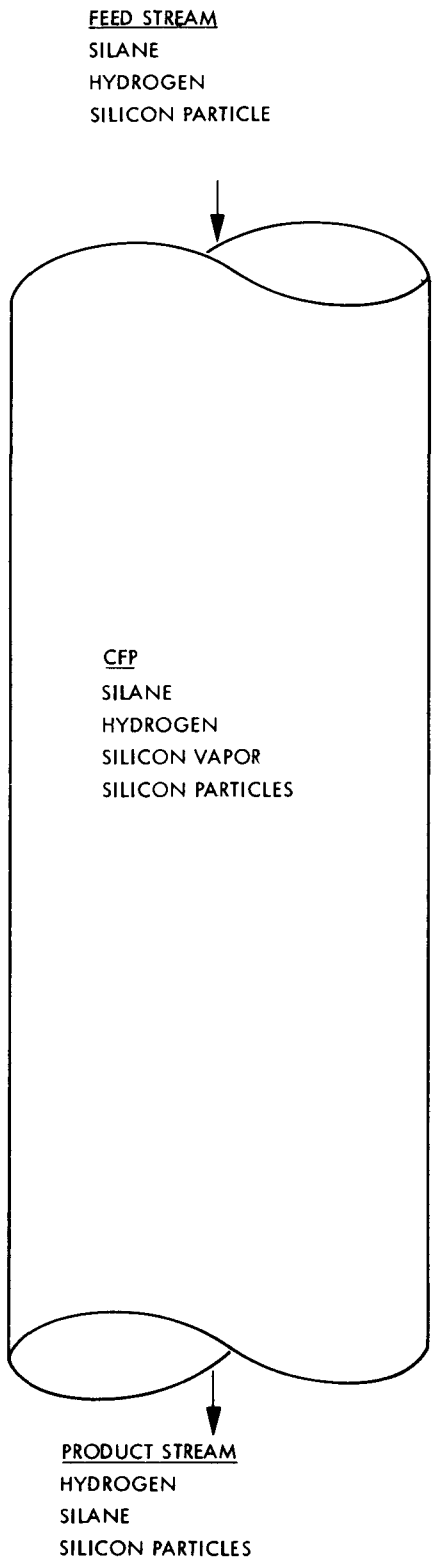

Figure 1-1. Silicon Production in a Continuous Flow Pyrolyzer

SECTION II

RATES OF SILANE PYROLYSIS

The physical picture of silane pyrolysis in the CFP can best be described as two-phase flow with simultaneous heat and mass transfer and chemical reactions. By any standards, this is a very complex problem for rigorous theoretical analysis. To solve the conservation equations for mass, momentum, and energy, it is necessary to know the rate of pyrolysis of silane in the CFP. In this section the rate equations for silane pyrolysis on silicon particles, on the reactor walls, and in the gas stream are developed. As mentioned previously, the silane pyrolysis reactions can be described by first-order Arrhenius type equations.

A. SILANE PYROLYSIS ON SURFACES

As shown in Figure 1-1, the pyrolysis reaction $SiH_4 \longrightarrow Si + 2H_2$ takes place in the CFP. It is assumed that the nucleation of silicon takes place instantaneously and that the silicon particles follow fluid motions. This means that there is no acceleration or radial diffusion of the silicon particles. Since the relative velocity between the gas and particles is zero, the visual image is one of a stagnant gas film surrounding each particle through which silane has to diffuse in order to arrive at the particle surface. The same assumption can be made for the reactor wall. For every mole of silane diffusing to the surface, there will be two moles of hydrogen diffusing back through the stagnant gas film:

$$2N_{si} = -N_h \tag{3}$$

The mass transfer between the bulk gas and the surface can be given by the Stefan-Maxwell relationship:

$$N_{si} = -CD_{AB}\left(\frac{dx_A}{dz}\right) + x_A\,(N_{si} + N_h) \tag{4}$$

Substituting equation 3 in equation 4,

$$N_{si} = \frac{-CD_{AB}}{1 + x_A}\,\frac{dx_A}{dz} \tag{5}$$

Following is a mass balance of silane over a thin slab of the gas film above the surface of thickness Δz:

$$SN_{si}\big|_z - SN_{si}\big|_{z + \Delta z} = 0$$

where S is the cross sectional area.

Dividing by S Δz and taking the limit as $\Delta z \longrightarrow 0$ gives

$$-\frac{dN_{si}}{dz} = 0 \tag{6}$$

Substituting equation 5 in equation 6,

$$\frac{d}{dz}\left(\frac{CD_{AB}}{1 + x_A}\frac{dx_A}{dz}\right) = 0 \tag{7}$$

Assuming that the total molal concentration and D_{AB} are constant in the thin film that surrounds the surfaces,

$$\frac{d}{dz}\left(\frac{1}{1 + x_A}\frac{dx_A}{dz}\right) = 0 \tag{8}$$

Integrating twice with respect to z gives

$$\ln (1 + x_A) = C_1 z + C_2 \tag{9}$$

The integration constants C_1 and C_2 can be evaluated with respect to the boundary conditions:

$$\text{at } Z = \delta,\ x_A = x_{AO}$$

$$\text{at } z = 0,\ x_A = x_{As}$$

The final result is

$$(1 + x_A) = 1 + x_{As}\left(\frac{1 + x_{AO}}{1 + x_{As}}\right)^{z/\delta} \tag{10}$$

Substituting equation 10 in equation 5, we obtain the rate of silane pyrolysis on surfaces:

$$N_{si} = \frac{CD_{AB}}{\delta} \ln \left(\frac{1 + x_{AO}}{1 + x_{AS}} \right) \tag{11}$$

Equation 11 provides the moles of silane pyrolyzed or moles of silicon deposited on surfaces per unit time per unit surface area. This equation is derived for the case of laminar flow in the CFP.

A very similar equation can be derived for turbulent flow in the CFP by assuming that enhancement in mass transfer can be accounted for by eddy diffusivity, ϵ_t. The final result is

$$N_{si} = \frac{C(D_{AB} + \epsilon_t)}{\delta} \ln \left(\frac{1 + x_{AO}}{1 + x_{AS}} \right) \tag{12}$$

Equations 11 and 12 may be written in terms of mass transfer coefficients, as the values of δ, ϵ_t and D_{AB} are difficult to determine. The mass transfer coefficients can be evaluated from correlations available in the literature (Reference 6). Equation 13 gives the rate of mass transfer of silane to surfaces, with the use of appropriate mass transfer coefficient.

$$N_{si} = k_m C \ln \left(\frac{1 + x_{AO}}{1 + x_{AS}} \right) \tag{13}$$

The reaction rate of silane pyrolysis on surfaces may be given by the equation

$$N_{si} = k_2 C_{si,s} \tag{13a}$$

At steady state conditions, the rates of mass transport and reaction are equal and hence the rate can be determined from the implicit relationship that can be derived by equating equations 13 and 13a.

$$e^{(N_{si}/k_m C)} = \frac{C + C_{si}}{C + (N_{si}/k_2)} \tag{14}$$

If silane mass transport is the controlling step ($C_{si,s} = 0$, $x_{AS} = 0$), the rate is given by the equation

$$N_{si} = k_m C \ln (1 + x_{AO}) \tag{15}$$

B. SILANE PYROLYSIS IN THE GAS STREAM

The rate of silane pyrolysis by the homogeneous mechanism can be determined from the equation

$$N_{si,H} = k_1 C_{si} \tag{16}$$

Equations 15 and 16 will therefore be used in the conservation equations to account for the loss of silane in the gas stream.

SECTION III

MATHEMATICAL MODELS OF SILANE PYROLYSIS

The axial profiles of gas velocity, temperature, and concentrations can be obtained by solving a set of differential equations that describe the conservation of momentum, mass and energy of the gas stream in the CFP. The solution of the simultaneous conservation equations for momentum, heat, and mass (Reference 6) gives the profiles of velocity, temperature, and concentrations as functions of the space coordinates and time. An analytical or even a numerical solution of these conservation equations is very difficult to obtain. For a complete solution for simultaneous momentum, heat and mass transfer in the CFP, seven simultaneous non-linear partial differential equations (3 equations of motion, 1 equation of energy, 2 equations of mass continuity, and the equation of state for the gaseous medium) must be solved for seven variables (3 velocity components, temperature, concentrations of silane and hydrogen, and density of the gas mixture). This is clearly a formidable task, even for a large computer. The equations are therefore simplified based on the six assumptions given in the previous section, the physical picture, and the silicon production process in the CFP.

A. ONE-DIMENSIONAL MODEL

The steady state, one-dimensional model that is developed here is based on macroscopic balances for momentum, mass, and energy. All of the independent variables in this simple model (velocity, temperature, and concentrations) are functions of the axial distance only. The elemental volume over which the macroscopic balances are made is shown in Figure 3-1. The macroscopic balances are based on the assumption that radial variations in velocity, temperature, and concentrations are insignificant in relation to their axial variations. The differential macroscopic balances can also be derived from the general equations of change given in Bird et al (Reference 6). Within the differential volume, silane is depleted by both the homogeneous and heterogeneous mechanisms. By the homogeneous mechanism, silane is pyrolyzed in the gas phase at a rate given by equation 16. By the heterogeneous mechanism, silane is pyrolyzed on the silicon particle surface and the reactor wall at a rate given by equation 15. Thus, the transport equations can be written in terms of the bulk mean values of the independent variables.

Equation of Motion

$$\rho V_{z,m} \frac{dV_{z,m}}{dz} = - \frac{dP}{dz} + g \qquad (17)$$

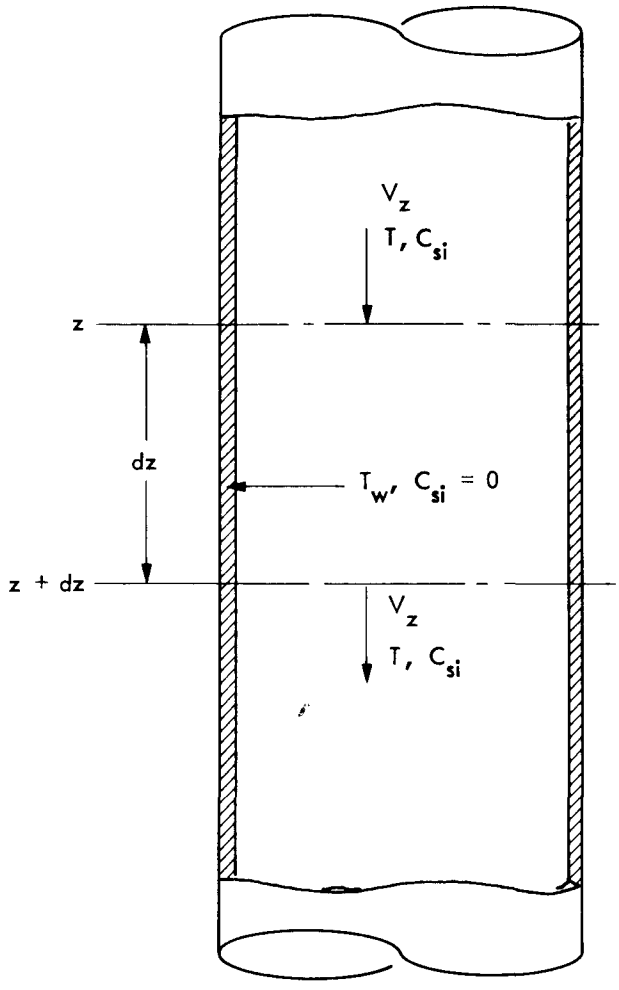

Figure 3-1. Differential Macroscopic Volume in the CFP

Equation of State

$$PV = nRT \tag{18}$$

$$\rho = C_{si,m} M_{si} + C_{h,m} M_h \tag{19}$$

Equation of Mass Continuity for SiH_4

$$\frac{d\,(V_{z,m}\, C_{si,m})}{dz} = -\epsilon N_{si,H} - N_{si}\,(\frac{2}{R} + ns) \tag{20}$$

Equation of Mass Continuity for Hydrogen

$$\frac{d(V_{z,m}\ C_{h,m})}{dz} = 2N_{si,H} + 2N_{si}\ (\frac{2}{R} + ns) \qquad (21)$$

Equation of Energy

$$\frac{d}{dz}\left(T_m\ V_{z,m}\ \left[\rho_m, C_{v,m} + mn\ C_{p,p}\right]\right) = \left(\epsilon N_{si,H} + N_{si} ns\right)\lambda$$

$$- \frac{2}{R} N_{si}\ \left(M_{si}\ C_{v,si}\ T_m - M_h\ C_{v,h}\ T_w\right) + \frac{2h}{R}\ (T_w - T_m) \qquad (22)$$

Equation of Mass Continuity for Silicon Seed Particles

$$nV_{z,m}\ \frac{dm}{dz} = N_{si,H}\ M_s + (\frac{6\sqrt{\pi m}}{\rho_p})^{2/3}\ N_{si}\ nM_s \qquad (23)$$

The differential equations 17, 20, 21, 22 and 23 are to be solved simultaneously to obtain the axial profiles of velocity, temperature, concentrations of silane and hydrogen, and particle mass. The initial conditions for the set of differential equations are:

at $z = 0$, $V_{z,m} = V_{z,i}$

$T_m = T_{m,i}$

$C_{si,m} = C_{si,i}$

$C_{h,m} = C_{h,i}$

$m = m_i$

The equation (23) of mass continuity for silicon seed particles assumes that all the silicon produced in the reactor (except for the amount deposited on the reactor wall) is deposited on the seed particles and that the seed particles are at the same temperature as the gas stream.

B. TWO-DIMENSIONAL MODEL

The second model developed here is a steady state, two-dimensional model based on conservation equations for momentum, mass, and energy. In this model, all the independent variables are functions of both the axial and radial distances. The two-dimensional model should reflect the actual conditions in the CFP more closely than the one-dimensional model, as the experiments at Union Carbide and JPL have shown the existence of radial gradients for temperature and concentrations. In the development of the model, the velocity components in the radial and circumferential directions are assumed to be zero.

It is assumed that the axial velocity (V_z), temperature (T), and concentrations of silane and hydrogen (C_{si}, C_h) are independent of θ, by virture of cylindrical symmetry. It can also be assumed that the variation of these variables in the axial direction is much smaller than their variation in the radial direction. With these assumptions, and neglecting viscous dissipation, the following equations can be derived from the set of equations given in Bird et al (Reference 6). These simplifications can be expressed mathematically as follows:

$$V_r = V_\theta = 0$$

$$\frac{\partial}{\partial\theta}(V_z,\ T,\ C_{si},\ C_h) = 0 \quad \text{(Cylindrical symmetry)}$$

$$\frac{\partial}{\partial t}(V_z,\ T,\ C_{si},\ C_h) = 0 \quad \text{(Steady state)}$$

$$r = N_{si}\ (\frac{2}{R} + ns) + N_{si,H} \quad \text{(Rate of silane conversion to silicon)}$$

$$\frac{\partial^2}{\partial z^2}\ (V_z,\ T,\ C_{si},\ C_h) << \frac{\partial}{\partial r}\ (r\frac{\partial}{\partial r}\ (V_z,\ T,\ C_{si},\ C_h))$$

$$(T{:}\Delta v) \approx 0 \quad \text{(Negligible viscous dissipation)}$$

$$K\Delta^2 T \approx 0 \quad \text{(Negligible heat-transfer by conduction)}$$

$$PV = nRT \quad \text{(Ideal gas)}$$

$$(\frac{\partial P}{\partial T})_\rho = \frac{P}{T}$$

The conservation equations can be simplified with these assumptions to the form given below.

Equation of Motion

$$\rho V_z \frac{\partial V_z}{\partial z} = \frac{1}{r} \frac{\partial}{\partial r}\left(r\mu \frac{\partial V_z}{\partial r}\right) - \left(\frac{\partial P}{\partial z}\right) + \rho g \qquad (24)$$

B.C. at $r = R$, $V_Z = 0$

at $r = 0$, $\frac{\partial V_z}{\partial r} = 0$

at $z = 0$, $V_z = V_{z,i}$

Equation of Energy

$$\rho C_p V_z \frac{\partial T}{\partial z} = \frac{1}{r} \frac{\partial}{\partial r}\left\{rk \frac{\partial T}{\partial r}\right\} - P \left\{\frac{\partial V_z}{\partial z}\right\}$$

$$- \left\{N_{si,H} + N_{si}\left(\frac{2}{R} + ns\right)\right\}\lambda \qquad (25)$$

B.C. at $r = R$, $T = T_W$

at $r = 0$, $\frac{\partial T}{\partial r} = 0$

at $z = 0$, $T = T_i$

Equation of Mass Continuity for SiH_4

$$V_z \frac{\partial C_{si}}{\partial z} = \frac{1}{r} \frac{\partial}{\partial r}\left(\frac{rD\partial C_{si}}{\partial r}\right) - N_{si,H} - N_{si}\left(\frac{2}{R} + ns\right) \qquad (26)$$

B.C. at $r = R$, $C_{si} = 0$

at $r = 0$, $\frac{\partial C_{si}}{\partial r} = 0$

at $z = 0$, $C_{si} = C_{si,i}$

Equation of Mass Continuity for H_2

$$V_z \frac{\partial C_h}{\partial z} = \frac{1}{r} \frac{\partial}{\partial r} \left(rD \frac{\partial C_h}{\partial r} \right) + 2N_{si,H} + 2N_{si} \left(\frac{2}{R} + ns \right) \qquad (27)$$

B.C. at $r = R$, $C_h = C$

at $r = 0$, $\frac{\partial C_h}{\partial r} = 0$

at $z = 0$, $C_h = C_{h,i}$

The four partial differential equations (equations 24-27) can be solved simultaneously on a computer using a numerical method based on finite differences. A numerical solution of these four coupled partial differential equations will yield the radial steady state profiles of temperatures, velocity, and concentration along the length of the reactor. The selection of a specific numerical algorithm depends on the stiffness of the partial differential equations and the accuracy needed. The bulk mean values of velocity, temperature, and concentrations at any given axial position can be obtained by integrating the radial profiles over the reactor cross section.

$$V_{zm} = \frac{\int_o^R V_z r dr}{\int_o^R r dr} = \frac{2\pi \int_o^R V_z r dr}{A} \qquad (28)$$

$$T_m = \frac{2\pi \int_o^R \rho C_p V_z T \, r dr}{V_{zm} A} \qquad (29)$$

$$C_{si,m} = \frac{2\pi \int_o^R V_z C_{si} r dr}{V_{zm} A} \qquad (30)$$

$$C_{h,m} = 1 - C_{si,m} \qquad (31)$$

The solution of equations 24-27 will be stopped at a reactor length at which the silane concentration ($C_{si,m}$) has reached a negligibly small value (0.1% of original value).

C. TURBULENT FLOW IN THE CFP

In the case of turbulent flow in the CFP, the conservation equations become much more complex and intractable. For turbulent flow, the velocity components exist in all three directions, and this in turn influences the heat and mass transfer. Thus, the complete set of conservation equations (continuity for silane and hydrogen, momentum for the three velocity components, equation of state for the gas, the energy equation, and overall mass continuity), a total of eight-nonlinear partial differential equations, have to be solved simultaneously to obtain instantaneous three-dimensional profiles of velocity, temperature, and concentrations. Alternately the set of equations can be time averaged and expressed in terms of time-mean quantities of velocity, temperature, and concentration. This would reduce the number of equations to six, since time-mean velocity components in the "r" and "θ" directions are zero. The equations would be very similar to those derived for the laminar case. However, the process of time averaging of equations results in the creation of three new variables: turbulent momentum, heat, and mass fluxes. It would be necessary to use three additional relationships to express the three turbulent fluxes in terms of the time-mean velocity, temperature, and concentration gradients. Thus, we can see that the solution of the conservation equations for the turbulent case may be very difficult and time consuming (even on a computer). It is therefore more fruitful to solve the turbulent case with the macroscopic balance approach (one-dimensional model).

D. IMPLEMENTATION OF THE MODEL

A computer program has been developed to implement the model of CFP based on macroscopic balances (one-dimensional model). A listing of the program is included as Appendix A. This computer program obtains a solution of the simultaneous differential equations 17, 20, 21, 22, and 23. These equations are non-dimensionalized so that all the time-dependent variables have the same order of magnitude. The new variables have been defined as follows:

$$Y_1 = \frac{Y_{z,i}}{V_{z,m}} \tag{32}$$

$$Y_2 = \frac{C_{si,m}}{C_{si,i}} \cdot \frac{1}{Y_i} \tag{33}$$

$$Y_3 = 1 + \left\{\frac{C_{h,i}}{2C_{si,i}}\right\} - \left\{\frac{C_{h,m}}{2C_{si,i}} \cdot \frac{1}{Y_1}\right\} \tag{34}$$

$$Y_4 = \frac{T_w - T_m}{T_w - T_{m,i}} \tag{35}$$

$$Y_5 = \frac{m_f - m}{m_f - m_i} \tag{36}$$

The final non-dimensionalized equations and their derivation are included in Appendix B. The computer program has been debugged and tested with data representative of the experimental conditions used in the JPL experiments.

SECTION IV

SUMMARY AND FUTURE PLANS

A. SUMMARY

1. Mathematical models of the effects of transport processes on silane conversion in the continuous flow pyrolyzer have been developed. The first model describes the silane conversion process by means of one-dimensional macroscopic balances for momentum, energy, and mass. The second model describes the process by means of two-dimensional conservation equations for momentum, energy, and mass.

2. The macroscopic balances model has been implemented as a computer program which predicts the axial velocity, temperature, and concentration profiles in the reactor, and overall rate of silane pyrolysis and seed particle growth.

B. FUTURE PLANS

1. The one-dimensional model will be modified to account for the creation and growth of silicon particles within the CFP via the homogeneous mechanism of silane pyrolysis and silicon nucleation. This modification is necessary because all of the silicon product obtained in the Union Carbide and JPL experiments is in the form of very fine particles. In the Union Carbide experiment seed particles were not used. In the JPL experiments growth on cold silicon seed particles was not observed. Thus, the proposed modification for nuclei will allow direct comparison of the experimental results on particle size with model predictions.

2. The energy balance equations of the models will be modified to allow for independent seed particle temperature. Hot silicon seed particles will be used in JPL experiments for the purpose of increasing the seed particle growth.

3. The boundary conditions used for the solution of the model equation will be modified to reflect the actual geometry of the CFP and the heating method used in JPL experiments. A co-axial thermowell rather than a constant temperature hot reactor wall is used to provide the heat in JPL experiments.

4. After the one-dimensional model is modified and tested with experimental data, the two-dimensional mathematical model will be implemented for a more precise modeling of silane pyrolysis in the CFP.

REFERENCES

1. Praturi, A. K., Proceedings of the Sixth International Chemical Vapor Deposition Conference (Eds., L. F. Donaghey, P. Rai-Choudhyry, and R. N. Tauber), p. 20-34, The Electrochemical Society, Inc., Princeton, New Jersey, 1977.

2. Praturi, A. K., Lutwack, R., and G. C. Hsu, Chemical Vapor Deposition of Silicon from Silane Pyrolysis, JPL Publication 77-38, 1977.

3. Everstiyn, F. C. and B. H. Put, J. Electrochem. Soc., 120, 1, 106-110, 1973.

4. McDonald, J. E., Amer. J. Phys., 31, 1, 31-41, 1963.

5. Farrow, R. F. C., J. Electrochem. Soc., 121, 7, 899-907, 1974.

6. Bird, R. B., Stewart, W. E., and E. N. Lightfoot, Transport Phenomena, John Wiley & Sons, Inc., New York, 1960.

APPENDIX A

LISTINGS OF THE COMPUTER PROGRAM FOR THE ONE-DIMENSIONAL MODEL

```
//SILICON  JOB (98908,RAJ,JPL),'RAVI',TIME=(00,20)
/*ROUTE  PRINT R3
//       EXEC  FORTG
//FORT   DD    *
       EXTERNAL CLIKN
       DIMENSION Y(4),YDOT(4)
       COMMON/TDPRM/A1,E1,A2,E2,HR
       COMMON/INICON/CAO,CBO,VIN,TIN,TW
       COMMON/REKTR/RA
       COMMON/PATICL/PMO,PNO,DSI,PCO,PC,PS,PV
       COMMON/HTRC/RATIO
       READ(5,10) A1,E1,A2,E2,HR
       READ(5,20) CAO,CBO,VIN,TIN,TW
       READ(5,30) RA
       READ(5,40) PMO,PNO,DSI
       READ(5,50) RATIO
 10    FORMAT(5F6.1)
 20    FORMAT(2E13.6,F7.3,2F7.1)
 30    FORMAT(F6.3)
 40    FORMAT(E13.6,F5.1,F6.3)
 50    FORMAT(F5.2)
       WRITE(6,60)
 60    FORMAT('0'/'0','INPUT DATA'/)
       WRITE(6,70) A1,E1,A2,E2,HR
 70    FORMAT('0'/'0','A1,E1,A2,E2,HR'/'0',5F6.1/)
       WRITE(6,80) CAO ,CBO,VIN,TIN,TW
 80    FORMAT('0'/'0','CAO,CBO,VIN,TIN,TW'/'0',2E13.6,F7.3,2F7.1/)
       WRITE(6,90) RA
 90    FORMAT('0'/'0','RA'/'0',F6.3/)
       WRITE(6,100) PMO,PNO,DSI
 100   FORMAT('0'/'0','PMO,PNO,DSI'/'0',F13.6,F5.1,F6.3)
       WRITE(6,110) RATIO
 110   FORMAT('0'/'0','RATIO OF HT TR COFFFS'/'0',F5.2)
       WRITE(6,900)
 900   FORMAT('0'///'0','OUTPUT'///)
       K1=0
       N=4
       T=0.001
       DO 1 I=1,4
 1     Y(I)=1.0
       DT=0.1
       EPS=1.0E-04
       K=1
 3     CALL MODDEQ(CLIKN,K,N,T,Y,YDOT,DT,EPS)
       IF(K.LT.0) GO TO 2
       IF(Y(2).LE.0.9.AND.Y(2).GE.0.89) K1=K1+1
       IF(Y(2).LE.0.8.AND.Y(2).GE.0.79) K1=K1+1
       IF(Y(2).LE.0.7.AND.Y(2).GE.0.69) K1=K1+1
       IF(Y(2).LE.0.6.AND.Y(2).GE.0.59) K1=K1+1
       IF(Y(2).LE.0.5.AND.Y(2).GE.0.49) K1=K1+1
       IF(Y(2).LE.0.4.AND.Y(2).GE.0.39) K1=K1+1
       IF(Y(2).LE.0.3.AND.Y(2).GE.0.29) K1=K1+1
       IF(Y(2).LE.0.2.AND.Y(2).GE.0.19) K1=K1+1
       IF(Y(2).LE.0.1.AND.Y(2).GE.0.09) K1=K1+1
       IF(K1.EQ.1) WRITE(6,4)K,T,Y
       K1=0
       IF(Y(2).GT.0.01) GO TO 3
 2     WRITE(6,4) K,T,Y
```

```
4     FORMAT('0'/'0','K= ',I3/'0','AXIAL DIST. Z=',E15.6,'  CM.'/'0','
     1 I              Y'/'0',' 1      ',E13.6/'0',' 2       ',E13.6/
     2'0',' 3       ',F13.6/'0',' 4       ',E13.6//)
      STOP
      END
      SUBROUTINE CLIKN(N,T,Y,YDOT)
      EXTERNAL F1,F2
      DIMENSION Y(4),YDOT(4)
      DIMENSION ROOTS(2),ITER(2),FRT(2)
      COMMON/TDPRM/A1,E1,A2,E2,HR
      COMMON/INICON/CA0,CB0,VIN,TIN,TW
      COMMON/REKTR/RA
      COMMON/PATICL/PM0,PN0,DSI,PC0,PC,PS,PV
      COMMON/HTRC/RATIO
      COMMON/SF/C,CA
      COMMON/SF1/RC2,CMT1
      COMMON/SF2/RC3,CMT2
      GR=1.987E-03
      GG=1.987
      GO=8.314E+07
      DT=TW-TIN
      TG=TW-DT*Y(3)
      C=Y(1)*CA0*(2.0+(CB0/CA0)-Y(2))
      CA=Y(1)*Y(2)*CA0
      CB=C-CA
      RC1=(10.0**A1)*EXP(-E1/(GR*TG)) *2.0
      RC2=(10.0**A2)*EXP(-E2/(GR*TG))*2.5
      RC3=(10.0**A2)*EXP(-E2/(GR*TW))*2.5
      PC0=(7.0*PN0)/(22.0*RA*RA*VIN)
      PC=PC0*Y(1)
      FM=(CA0*28.0)/PC0+PM0
      PM=FM-(FM-PM0)*Y(4)
      PS=((6.0*SQRT(22.0/7.0)*PM)/DSI)**0.6666
      PV=PM/DSI
      VOID=1.0-PV*PC
      RP=((3.0*PV)/(4.0*3.143))**0.3333
      DIFU=1.25086E-04*(TG**1.5)
      DO 10 I=1,2
      TG1=TG
      IF(I.EQ.2) TG1=TG+0.5*(TW-TG)
      VISA=((TG1/288.0)**1.5)*(524.67/(TG1+236.67))*(11.24E-05)
      VISB=((TG1/293.0)**1.5)*(322.841/(TG1+29.841))*(8.8E-05)
      VIS=VISA/(1.0+(((CB/CA)*(1.0+((VISA/VISB)**0.5)*0.5)**2)/16.6619))
     1+VISB/(1.0+(((CA/CB)*(1.0+((VISB/VISA)**0.5)*2.0)**2)/2.915476))
      IF(I.EQ.1) VISS=VIS
      RE=(2.0*RA*(32.0*CA+2.0*CB)*VIN)/(VISS*Y(1))
      K=0
      IF(RE.GT.2100.0) K=1
      CPA=(0.2233+(1.323E-04)*TG1+(61.94E-08)*(TG1**2) )*32.0
      CPB=     (6.52+(0.78E-03)*TG1+(0.12E+05)/(TG1**2))
      CP=(CA*CPA+CB*CPB)/C
      IF(I.EQ.1) CV=C*(CP-GG)/(CA*32.0+CB*2.0)
      IF(I.EQ.1) CVA=(CPA-GG)/32.0
      IF(I.EQ.1) CVB=(CPB-GG)/2.0
10    CONTINUE
      CMT1=DIFU/RP
      RAT=CMT1*C*PS*PC*ALOG(1.0+(CA/C))
      SC= VIS/((32.0*CA+2.0*CB)*DIFU)
```

```
      RE=(2.0*RA*(32.0*CA+2.0*CB)*VIN)/(VIS*Y(1))
      CMT2=(DIFU/(2.0*RA))*(3.65+((0.0668*((2.0*RA)/T)*RE*SC)/(1.0+0.04*
     1(((2.0*RA)/T)*RE*SC)**0.6666)))
      RATE=(CMT2*C*2.0*ALOG(1.0+(CA/C)))/RA
      TCA=VISA*(CPA+2.48)/32.0
      TCB=0.002389*(0.080796+(3.7312E-04)*TG1-(7.4683E-09)*TG1*TG1)
      TC=(CA*TCA*(32.0**0.3333)+CB*TCB*(2.0**0.3333))/(CA*(32.0**0.3333)
     1+CB*(2.0**0.3333))
      PR=(C*CP*VIS)/(TC*(CA*32.0+CB*2.0))
      IF(K.EQ.1) GO TO 20
      HT=(TC/(2.0*RA))*(3.65+((0.0668*(2.0*RA/T)*RE*PR)/(1.0+0.04*(((2.0
     1*RA/T)*RE*PR)**0.6666))))
      GO TO 30
20    FR=0.316/(RE**0.25)
      HT=(TC/(2.0*RA))*RE*PR*((FR/2.0)/(1.07+12.7*SQRT(FR/2.0)*(PR**0.66
     166-1.0)))
30    HTR=RATIO*HT
      HT=HT+HTR
      PCP=(5.74+0.000617*TG-(101000.0/(TG**2)))/28.0
      SIL1=2.0*(1.0+CB0/(2.0*CA0))
      SIL2=(G0*TG*(Y(1)**2))/((Y(2)*32.0+(SIL1-2.0*Y(2))*2.0)*(VIN**2))
      SIL3=1.0-SIL2*(SIL1-Y(2))
      SIL4=(G0*(SIL1-Y(2))*DT*(Y(1)**3))/((Y(2)*32.0+(SIL1-2.0*Y(2))*2.0
     1)*(VIN**2))
      SIL5=-DT*(CV*(Y(2)*CA0*VIN*32.0+(SIL1-2.0*Y(2))*CA0*VIN*2.0)+(FM-(
     1FM-PM0)*Y(4))*PC*PCP*(VIN/Y(1)))
      YDOT(1)=-(SIL2/(SIL3*VIN))*Y(1)*(-RC1*VOID*Y(1)*Y(2)-(RAT      )/CA0
     10-(RATE     )/CA0)-(SIL4/(SIL3*SIL5))*((RC1*VOID*Y(1)*Y(2)*CA0+RAT
     2     )*(HR+TG*28.0*(CV-PCP))+RATE     *(CV*TG*28.0+4.0*CVR*TW-32.0*
     3CVA*TG))-(980.0*(Y(1)**3))/(VIN*VIN*SIL3)
      YDOT(2)=-(1.0/VIN)*(RC1*VOID*Y(1)*Y(2)+(RAT/CA0)      +(1.0/CA0)*
     1RATE)
      YDOT(3)=(1.0/SIL5)*((RC1*VOID*Y(1)*Y(2)*CA0+RAT      )*(HR+TG*28.0*
     1(CV-PCP))+RATE     *(CV*TG*28.0+4.0*CVR*TW-32.0*CVA*TG))
      YDOT(4)=-(28.0/(PC0*VIN*(FM-PM0)))*(RC1*VOID*Y(1)*Y(2)*CA0+RAT)
      RETURN
      END
      FUNCTION F1(X)
      COMMON/SF/C,CA
      COMMON/SF1/RC2,CMT1
      COMMON/PATICL/PM0,PN0,DSI,PC0,PC,PS,PV
      F1=(1.0+X)*EXP((RC2*X)/(CMT1*PS*PC))-(1.0+CA/C)
      RETURN
      END
      FUNCTION F2(X)
      COMMON/SF/C,CA
      COMMON/SF2/RC3,CMT2
      COMMON/REKTR/RA
      F2=(1.0+X)*EXP((RC3*X*RA)/(CMT2*2.0))-(1.0+CA/C)
      RETURN
      END
//DATA   DD     *
  12.0  36.0   6.0  17.05200.0
 3.069240E-06 5.831556E-05  4.572  298.0 1073.0
 2.858
 2.438922E-04 68.0 2.329
 1.00
//
```

APPENDIX B

NON-DIMENSIONALIZATION OF THE ONE-DIMENSIONAL MODEL EQUATIONS

This appendix discusses the non-dimensionalization of differential equations 17, 20, 21, 22, and 23 in this report. Non-dimensionalization is important for smooth integration.

New dimensionless variables were defined in equations 32, 33, 34, 35, and 36 as:

$$Y_1 = \frac{V_{z,i}}{V_{z,m}} \tag{A1}$$

$$Y_2 = \frac{C_{si,m}}{C_{si,i}} \quad \frac{1}{Y_1} \tag{A2}$$

$$Y_3 = 1 + \frac{C_{h,i}}{2C_{si,i}} - \frac{C_{h,m}}{2C_{si,i}} \quad \frac{1}{Y_1} \tag{A3}$$

$$Y_4 = \frac{T_w - T_m}{T_w - T_{m,i}} \tag{A4}$$

$$Y_5 = \frac{m_f - m}{m_f - m_i} \tag{A5}$$

where m_f = mass/particle if all the silane in the feed reacts and all the silicon produced is deposited on the particles. Using a simple mass balance,

$$\pi R^2 V_{z,i} C_{si,i} M_s = \pi R^2 V_{z,1} n_1 m_f - \pi R^2 V_{z,i} n_i m_i \tag{A6}$$

Since (for the particles)

$$\frac{d}{dt} (n \cdot V_{z,m}) = 0$$

or

$$n_z V_{z,m} = n_i V_{z,i}$$

therefore

$$n_1 V_{z,1} = n_i V_{z,i} \tag{A7}$$

Using equations A6 and A7

$$m_f = \frac{C_{si,i}\, M_s}{n_i} + m_i \tag{A8}$$

The differential equations can now be written in terms of the new dimensionless variables. Equations 17, 18, and 19 reduce to

$$\frac{dY_1}{dz} = \frac{f_o(Y)}{f_1(Y)}\, Y_1\, \frac{dY_2}{dz} - 2\, \frac{f_o(Y)}{f_i(Y)}\, Y_1\, \frac{dY_3}{dz}$$

$$- \frac{f_{2(Y)}}{f_1(Y)}\, \frac{dY}{dz} - \frac{g}{V_{z,i}^2}\, \frac{1}{f_1(Y)}\, Y_1^3 \tag{A9}$$

where

$$f_o(Y) = \frac{Rg\ T_w - (T_w - T_{m,i})\, Y_4\ Y_1^2}{Y_2\, M_{si} + (A - 2Y_3)\, M_h\ V_{z,i}^2} \tag{A10}$$

$$A = 2\ (1 + \frac{C_{h,i}}{2C_{si,i}}) \tag{A11}$$

$$f_1\ (Y) = 1 - f_o(Y)\ (A + Y_2 - 2Y_3) \tag{A12}$$

$$f_2(Y) = \frac{Rg\ (Y_2 + A - 2Y_3)\ (T_w - T_{m,i})}{Y_2\, M_{si} + (A - 2Y_3)\, M_h}\ \ \frac{Y_1^3}{V_{z,i}^2} \tag{A13}$$

Equations 20 and 21 reduce to

$$\frac{dY_2}{dz} = - \frac{k_1}{V_{z,i}}\, Y_1 Y_2 - \frac{N_{si}}{C_{si,i}\, V_{z,i}}\, (\frac{2}{R} + ns) \tag{A14}$$

and

$$\frac{dY_3}{dz} = -\frac{k_1^{\epsilon}}{V_{z,i}} Y_1 Y_2 - \frac{N_{si}}{C_{si,i}\, V_{z,i}} \left(\frac{2}{R} + ns\right) \qquad (A15)$$

Thus

$$\frac{dY_2}{d_z} = \frac{dY_3}{d_z}$$

This is not surprising, since examination of the definition of Y_2 and Y_3 reveals that both define (1 - conversion) or "degree of completion":

$$Y_2 = \frac{\pi R^2\, V_{z,m}\, C_{si,m}}{\pi R^2\, V_{z,i}\, C_{si,i}} = 1 - \text{conversion}$$

$$= 1 - \frac{\pi R^2\, C_{h,m}\, V_{z,m} - \pi R^2\, C_{h,i}\, V_{z,i}}{2\pi R^2\, V_{z,i}\, C_{si,i}} = Y_3$$

Equation 22, after some manipulation, reduces to

$$\frac{dY}{dz} = \frac{1}{A_o} \Big[(K_1^{\epsilon}\, Y_1 Y_2\, C_{si,i} + N_{si}\, ns)(\lambda + (T_w - (T_w - T_{m,i})\, Y_4)\, (M_s)$$

$$(C_{v,m} - C_{p,p}) + N_{si}\, \frac{2}{R}\, (C_{v,m}\, (T_w - (T_w - T_{m,i})\, Y_4)\, M_s$$

$$+ 2\, M_h\, C_{v,h}\, T_w - M_{si}\, C_{v,si}\, (T_w - (T_w - T_{m,i})\, Y_4\,)\Big] \qquad (A16)$$

where

$$AO = -(T_w - T_{m,i}) \Big[C_{v,m}\, (Y_2\, C_{si,i}\, V_{z,i}\, M_{si} + (A - 2Y_3)$$

$$C_{si,i}\, V_{z,i}\, M_{si}) + (m_f - (m_f - m_i)\, Y_5)\, n\, C_{p,p}\, \frac{V_{z,i}}{Y_1}\Big] \qquad (A17)$$

And finally, equation 23 becomes

$$\frac{dY_5}{dz} = - \frac{M_s}{n_i V_{z,i} (m_f - m_i)} \quad (k_1^{\epsilon} \quad Y_1 Y_2 \, C_{si,i} + N_{si} \, ns) \qquad (A18)$$

Substituting in Y_1, equation A9, can be rewritten using equations A14, A15, and A16.

Thus, since $Y_2 = Y_3$, we have four equations in four unknowns.

$$\frac{dY_1}{dz} = -\frac{f_o(Y)}{f_1(Y)} Y_1 \left[\frac{k_i^{\epsilon}}{V_{z,i}} Y_1 Y_2 - \frac{N_{si} \, ns}{C_{si,i} V_{z,i}} - \frac{N_{si} \quad 2/R}{C_{si,i} V_{z,i}}\right]$$

$$- \frac{f_2(Y)}{f_1(Y)} \frac{1}{AO} \left[(k_1^{\epsilon} \quad Y_1 Y_2 \, C_{si,i} + N_{si} \, ns)(\lambda + (T_w - (T_w - T_i) Y_4) M_s\right.$$

$$(C_{v,m} - C_{p,p}) + N_{si} \frac{2}{R} (C_{v,m} (T_w - (T_w - T_i) Y_4) M_s +$$

$$\left. 2 M_h C_{v,h} T_w - M_{si} C_{v,si} (T_w - (T_w - T_i) Y_4)\right] - \frac{9}{V_{z,i}^2} \frac{1}{f_1(Y)} Y_1^3$$

$$\frac{dY_2}{dz} = - \frac{k_i^{\epsilon}}{V_{z,i}} Y_1 Y_2 - \frac{N_{si}}{C_{si,i} V_{z,i}} (\frac{2}{R} + ns)$$

$$\frac{dY_4}{dz} = \frac{1}{AO} \left[(k_1^{\epsilon} \quad Y_1 Y_2 \, C_{si,i} + N_{si} \, ns)(\lambda + (T_w - (T_w - T_{m,i}) Y_4) M_s\right.$$

$$(C_{v,m} - C_{p,p}) + N_{si} \frac{2}{R} (C_{v,m} (T_w - (T_w - T_{m,i}) Y_4) M_s$$

$$\left. + 2 m_h C_{v,h} T_w - M_{si} C_{v,si} (T_w - (T_w - T_{m,i}) Y_4)\right]$$

$$\frac{dY_5}{dz} = - \frac{M_s}{n_i V_{z,i} (m_f - m_i)} (k_1^{\epsilon} \quad Y_1 Y_2 \, C_{si,i} + N_{si} \, ns)$$

The initial conditions are:

at $z = 0$

$$Y_1 = Y(1) = 1.0$$
$$Y_2 = Y(2) = 1.0$$
$$Y_4 = Y(3) = 1.0$$
$$Y_5 = Y(4) = 1.0$$

To use this model, expressions for heat and mass transfer coefficients are needed.

Convective Heat Transfer Coefficient:

Expression 7-142 from Eckert & Drake, "Analysis of Heat and Mass Transfer" is used.

$$Nu_d = 3.65 + \frac{0.0668\ (d/x)\ Re_d Pr}{1 + 0.06\ \left[(d/x)\ Re_d Pr\right]^{2/3}}$$

for $Re \leq 2100$

For turbulent flow, expression for 'St' given on page 383 of the same book is used.

$$St = \frac{Nu_d}{Re_d Pr} = \frac{f/2}{1.07 + 12.7\sqrt{f/2}\ (Pr^{2/3} - 1)}$$

where

$$f = \frac{0.316}{(Re_d)^{1/4}}$$

In both cases, various properties (e.g. viscosity) are calculated at a reference temperature given by expression 7-86 of the same book in accordance with the discussion on page 341.

Radiative Heat Transfer Coefficient:

Assumed to be equal to convective heat transfer coefficient.

Particle-Gas Mass Transfer Coefficient:

Since the seed particles are assumed to follow the gas velocity, the dynamic picture is similar to that of particles in a stagnant gas, a case for which Nu = 2; hence, by analogy

$$Sh = 2$$

or

$$\frac{Kd}{D} = 2$$

where K = mass transfer coefficient

d = particle diameter

D = diffusisity

Wall-Gas Mass Transfer Coefficient:

The same expression as that for convective heat transfer coefficient is used with the following substitution:

Sh for Nu

Sc for Pr

Mixture properties such as viscosity, heat capacity, and thermal conductivity are calculated as functions of temperature and concentration at each step of integration.